17 Stable Isotope Geochemistry on the Intrusive Complex and Its Metamorphic Aureole

S. Hoernes, S. MacLeod-Kinsel, R.S. Harmon, D. Pattison and D.F. Strong

17.1 Introduction

Variations in stable isotope ratios can be particularly helpful in studying the origins of igneous rocks, as well as the fluid interactions that may accompany magma generation or which may occur during and after magma emplacement and solidification (see e.g., the recent review in Valley et al. 1986). In certain instances, and to certain extents, granitic magmas may inherit and preserve the isotopic composition of their source region (O'Neil and Chappel 1977; O'Neil et al. 1977; Chivas et al. 1982; Vidal et al. 1984; Hill et al. 1986). More commonly, mafic partial melts may interact with isotopically evolved crust during magma ascent through AFC-type processes which produce correlated stable-radiogenic isotope covariations within genetically related plutonic suites (Michard-Vitrac et al. 1980; Halliday et al. 1980; Clayburn et al. 1983; Fleck and Criss 1985). Finally, interaction with externally derived fluids at either magmatic or subsolidus stages can be an important process (Friedman et al. 1964; Forester and Taylor 1976, 1977; Hildreth et al. 1984; Fourcade and Javoy 1985; Wickham and Taylor 1987; Bickle et al. 1988).

Despite the fact that there are many unaltered granites with primary $\delta^{18}O$ values in excess of +10‰$_{SMOW}$, particularly within the Hercynian of western Europe (Sheppard 1977; Albarede et al. 1980; Michard-Vitrac et al. 1980; Bernard-Griffiths et al. 1985; Wickham and Taylor 1985), most granitoids worldwide have $\delta^{18}O$ values of +6 to +10‰$_{SMOW}$ and δD values of –90 to 40‰$_{SMOW}$ (Taylor 1968, 1974, 1977; O'Neil and Chappell 1977; O'Neil et al. 1977; Harmon and Halliday 1980; Solomon and Taylor 1981; Masi et al. 1981; Blattner et al. 1983; Xu et al. 1984). Generally, lower O- and H-isotope ratios, or internal mineral ^{18}O disequilibrium, are considered to be a reflection of interaction with an external fluid reservoir of different isotopic composition (e.g., magmatic or subsolidus exchange with meteoric hydrothermal fluids or hydrothermally altered country rocks). However, low δD values can also be produced by magma degassing during cooling and crystallization (Nabelek et al. 1983; Taylor et al. 1983).

This work examines the $^{18}O/^{16}O$ and D/H systematics of rocks and minerals of the Caledonian-age Ballachulish Igneous Complex and thermal metamorphic aureole in southwestern Scotland. Previous stable isotope work on Caledonian plutonic rocks of the Scottish Highlands is quite general in scope. On a regional scale, Harmon and Halliday (1980) and Harmon et al. (1984) observed a wide range of O-isotope variation ($\delta^{18}O$ = +7.2 to +11.0‰$_{SMOW}$), but small range of H-isotope variation (δD

G. Voll, J. Töpel, D.R.M. Pattison, F. Seifert
Equilibrium and Kinetics
in Contact Metamorphism
©Springer-Verlag Berlin Heidelberg 1991

17.8 Conclusions

The stable isotope data presented in this study have demonstrated that a granitoid magma, intruding at upper crustal levels, does not necessarily promote large hydrothermal convection cells which transport heat from the cooling intrusive body into the country rocks. This is most likely due to: (1) the low permeability and low H_2O-content of the host regional greenschist-amphibolite metamorphic country rocks; and (2) to the two-stage intrusion of the Ballachulish intrusive complex, where the first, relatively dry melts sealed the contact between the second stage, wet granitic magma and the country rocks. Thus, as a whole, the heat transfer was mainly carried out by heat conduction. Any substantial large-scale transport of matter via fluids from the pluton into the laterally adjacent sedimentary country rocks appears unlikely. The stable isotope data allow constraints on the petrogenesis of the magma: the parental mafic magma probably originated from the deep lower crust or the crust-mantle boundary area where it interacted with higher ^{18}O crust through a MASH-type process. Further modification occurred by combined fractional crystallization-assimilation processes during magma transit through and during residence in high-^{18}O upper crust prior to crystallization and cooling. This process was most likely responsible for the large variation in O-isotope composition of the phase II intrusion.

Some of the mineral phases which crystallized from the melt subsequently re-equilibrated during cooling at subsolidus conditions with a fluid phase exsolved from the crystallizing magma. The near equilibrium fractionations at lower temperatures than expected from closure temperatures of the particular minerals indicate a solution-redeposition process as a mechanism for O-isotope exchange. Only in rocks, which cooled in absence of an aqueous fluid phase, as indicated by the lack of retrograde phase transformations, can be observed a fractionation pattern typical for diffusive exchange.

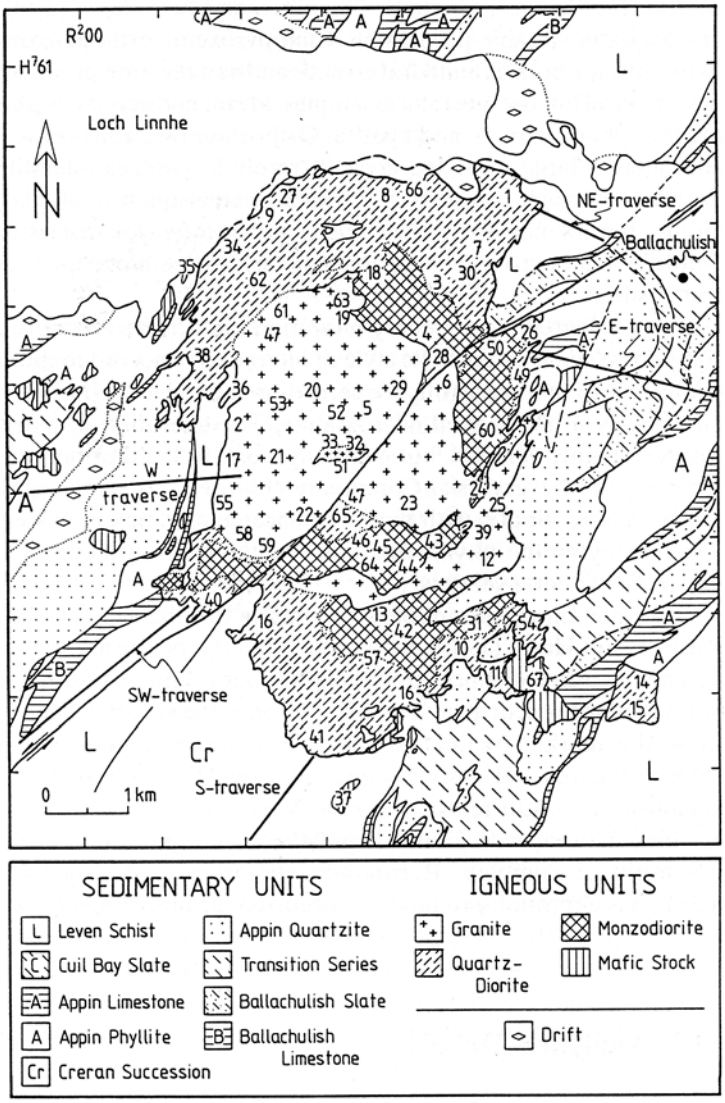

Fig. 17.1. Geological map of the Ballachulish igneous complex and its country rocks, indicating the locations of the igneous samples and of the country rock traverses discussed in this study. *Numbers* refer to samples listed in Table 17.1. SW traverse-D: samples DP83-30, DP358 and DP356; SW traverse-B samples with numbers 13898-13967 listed in Table 17.3

cuts completely through it from NE to SW. Country-rock xenoliths are common in the marginal phases of the intrusive complex.

The mineralogy of the Ballachulish igneous rocks is dominated by plagioclase (25–50 vol%) and alkali feldspar is estimated by Weiss and Troll (Chap. 4, this Vol.) to have constituted 10–20 vol% of the granitic melt at the time of emplacement.

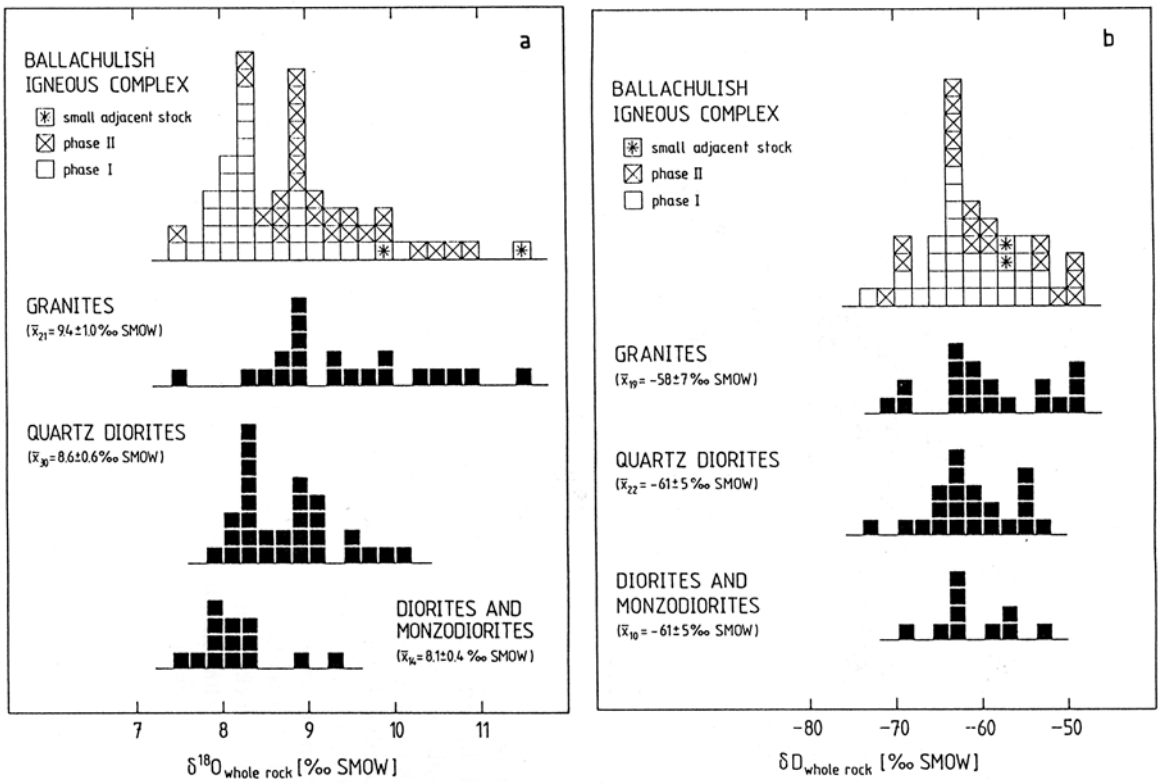

Fig. 17.2. Histograms of whole-rock $\delta^{18}O$ (**a**) and δD (**b**) distributions within the igneous complex. The large range of $\delta^{18}O$ variation (4‰) contrasts sharply with the small range of δD variation (25‰). Although there is no essential difference in D/H between rocks of different composition or intrusive phase, there are systematic variations in $^{18}O/^{16}O$ ratios. In general, there is a tendency for $^{18}O/^{16}O$ ratios to increase with the degree of chemical evolution and for rocks of the first intrusive phase to be less ^{18}O-rich than those of the second phase. A small quartz diorite-granite stock located about 1 km southeast of the main intrusive body is characterized by the highest $\delta^{18}O$ value measured in this study

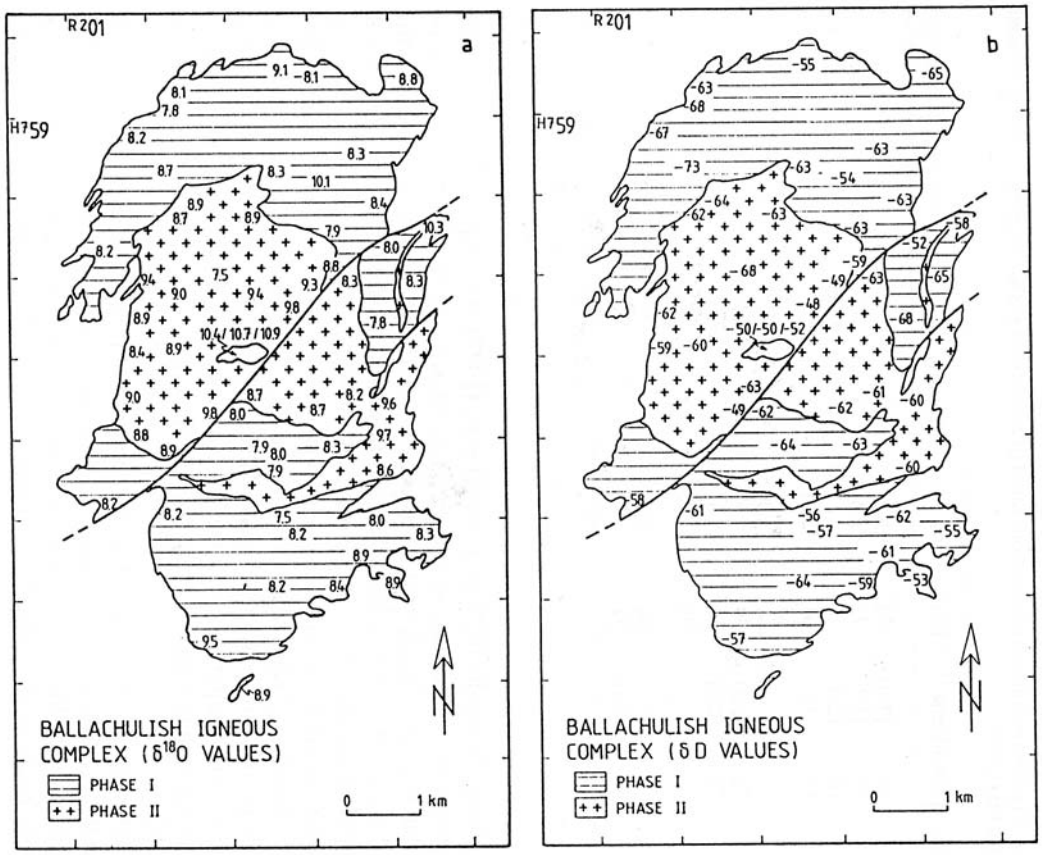

Fig. 17.3. Outline maps of the igneous complex illustrating the geographic distribution of whole-rock $\delta^{18}O$ values (**a**) and δD values (**b**). Note that there are no well-defined spatial patterns of isotopic variation

Table 17.3. Stable isotope compositions of metasedimentary rocks of the aureole[a]

Area/ traverse	Sample No.	Rock type	Aureole zone	Contact dist. (m)	$\delta^{18}O$ (‰SMOW)	δD	$\delta^{13}C$ (‰PDB)	H_2O^+ (wt%)
SW	DP641	Leven schist	IVb	550	+12.0	–45		2.5
SW	DP358	Leven schist	III	900	+11.0	–40		3.8
SW	DP356	Leven schist	I	1300	+11.1	–46		3.9
S	13898	Xenolith	V		+ 9.7			
S	13911	Leven schist	V	0.3	+11.0			
S	13913	Leven schist	V	10	+11.4			
S	13921	Leven schist	V	35	+11.5			
S	13924	Leven schist	V	100	+11.4			
S	13933	Leven schist	IV	220	+12.4			
S	13936	Leven schist	IV	235	+12.8			
S	13940	Leven schist	IV	240	+12.5			
S	13943	Leven schist	IV	290	+12.5			
S	13946	Leven schist	III	430	+12.0			
S	13951	Leven schist	II	510	+12.8			
S	13954	Leven schist	I	563	+11.2			
S	13954	Leven schist	I	610	+13.7			
S	13955	Leven schist	I	627	+12.3			
S	13963	Leven schist	I	680	+12.4			
S	13967	Leven schist	I	800	+14.3			
S	13970	Leven schist	I	894	+11.1			
S	13975	Leven schist	I	1010	+12.5			
S	13978	Leven schist	I	1240	+12.7			
S	DP626	Leven schist	V	100	+11.6	–52		1.9
S	DP627	Leven schist	IVb	200	+11.9	–50		1.7
S	DP377	Leven schist	III	320	+11.3	–51		2.8
S	DP629	Leven schist	I	670	+11.4	–52		3.9
S	V-LC	Leven schist		13000	+11.7			
W	DP5	Leven schist	V	50	+ 9.3	–55		4.0
W	DP5	Leven schist	V	30	+10.9	–53		2.8
W	A67-1	Lsh-leucosome	V		+11.5			
W	A67-11	Lsh-paleosome	V		+12.2			
W	A93-1	Lsh-leucosome	V		+11.6			
W	A93-2	Lsh-paleosome	V		+12.2			
W	SK29-13	Appin quartzite	IVb		+10.7			
W	SK29-11	Appin phyllite	III		+12.0	–43		2.8
W	SK29-10	Appin quartzite	II		+12.0			
W	DP16	Appin phyllite	I	3200	+14.0	–39		3.3
W	B5	Appin phyllite			+10.6			
W	B20	Appin quartzite		3000	+12.5			
W	B22	Appin quartzite		2800	+11.5			
W	B9	Appin quartzite		150	+11.0			
W	B41	Appin quartzite		100	+12.0			
W	B45	Appin quartzite		30	+12.2			
W	B44	Appin quartzite		25	+12.3			
W	B43	Appin quartzite		5	+12.3			
NE	DP49	Leven schist	V	20	+10.0	–52		2.4
NE	DP50	Leven schist	IVb	150	+ 9.3	–47		4.5
NE	DP482	Leven schist	I	700	+11.3	–53		2.7
NE	DP157	Leven schist	I	850	+11.8	–56		2.7
E	DP601	Appin phyllite	Vb	40	+12.7	–38		4.1
E	DP42	Appin phyllite	IVb	280	+12.9	–56		1.4

Table 17.3. (continued)

Area/ traverse	Sample No.	Rock type	Aureole zone	Contact dist. (m)	$\delta^{18}O$ (‰SMOW)	δD	$\delta^{13}C$ (‰PDB)	H_2O^+ (wt%)
E	DP22	Appin phyllite	IVb	500	+12.1	–55		1.7
E	DP505	Appin phyllite	IVb	550	+13.0	–51		2.6
E	SK01-5	Appin quartzite			+12.2			
E	SK01-6	Appin quartzite			+12.3			
E	SK01-7	Appin quartzite			+13.6			
E	SK01-8	Appin quartzite			+14.0			
E	DP125	Appin phyllite	III		+12.4	–62		2.4
E	DP134A	Appin phyllite	II		+13.4	–56		3.1
E	DP140	Appin phyllite	I		+15.2	–55		2.1
E	DP104	Appin phyllite	I		+14.1	–60		3.3
E	SH150	Dol. marble		700	+19.6		+2.7	
E	SH230	Dol. marble		620	+18.7		+3.8	
E	SH426	Dol. marble		600	+17.6		+3.2	
E	SH435	Dol. marble		430	+22.3			
E	SH307	Dol. marble		410	+19.3			
E	SH309	Dol. marble		350	+19.4		+2.3	
E	SH312	Dol. marble		250	+21.1		+4.4	
E	SH429	Dol. marble		140	+21.0		+3.2	
E	SH314	Dol. marble		100	+21.5		+3.0	
E	SH315	Dol. marble		70	+22.0		+3.8	
E	SH316	Dol. marble		40	+19.4			
E	SH317	Dol. marble		25	+21.4		+3.2	
E	SH421	Calc-silicate rock		790	+14.2		+2.3	
E	SH221	Calc-silicate rock		740	+13.3		–1.0	
E	SH223	Calc-silicate rock		715	+16.8		+3.0	
E	SH224	Calc-silicate rock		640	+16.8		+1.9	
E	SH225	Calc-silicate rock		535	+19.4		+2.7	
E	SH310	Calc-silicate rock		450	+16.0		+2.5	
E	SH311	Calc-silicate rock		390	+16.3		+3.7	
E	SH226	Calc-silicate rock		385	+15.6		+3.3	
E	SH227	Calc-silicate rock		235	+16.4		–0.8	
E	SH228	Calc-silicate rock		230	+16.6		+1.8	
E	SH428	Calc-silicate rock		170	+15.2		–1.4	
E	SH229	Calc-silicate rock		75	+16.7		+1.9	
E	W305	Psammopelite		430	+13.4			
E	W304	Psammopelite		340	+13.5			
E	SH379a	Pelite		330	+14.7			
E	SH379b	Psammopelite		330	+14.3			
E	W293	Psammopelite		265	+12.5			
E	W294	Psammopelite		245	+13.7			
E	W295a	Pelite		210	+15.2			
E	W295b	Psammopelite		210	+14.3			
E	W297a	Pelite		70	+16.1			
E	W297b	Psammopelite		70	+14.3			
E	W298	Pelite		10	+14.8			

[a]Metamorphic zones labelled after Pattison and Harte (1985).
Abbreviations: dol = dolomitic; Lsh = Leven schist; LC = Leven schist from Crearan Inn, Loch Crearan.

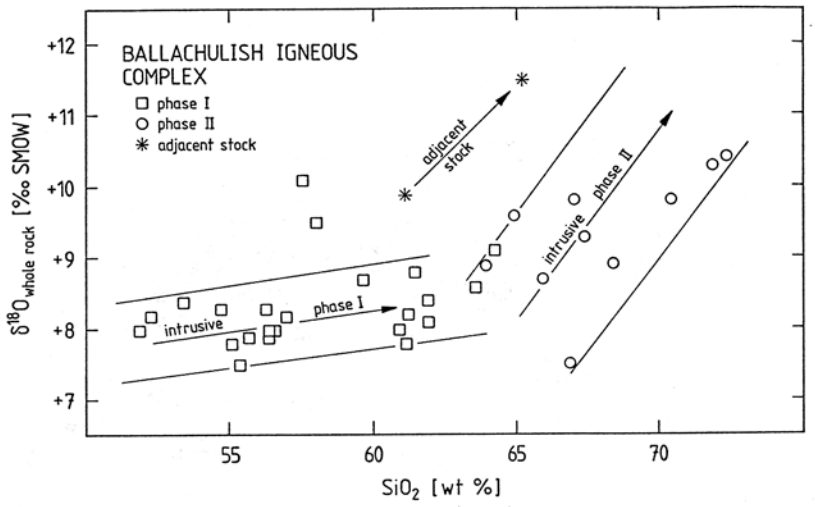

Fig. 17.4. Plot of whole-rock $\delta^{18}O$ values as a function of bulk composition as indicated by SiO_2 content. With three exceptions (DP217, DP460, and WT83), $\delta^{18}O$ values for the samples of each intrusive phase tend to increase systematically with changing bulk composition. The different *slopes* for each sample group suggests a lack of interaction or isotopic communication during emplacement and cooling. The steeper trends for the phase II rocks implies either a greater degree of contamination by a ^{18}O-rich crustal reservoir or assimilation and exchange with a different and more ^{18}O-rich contaminant

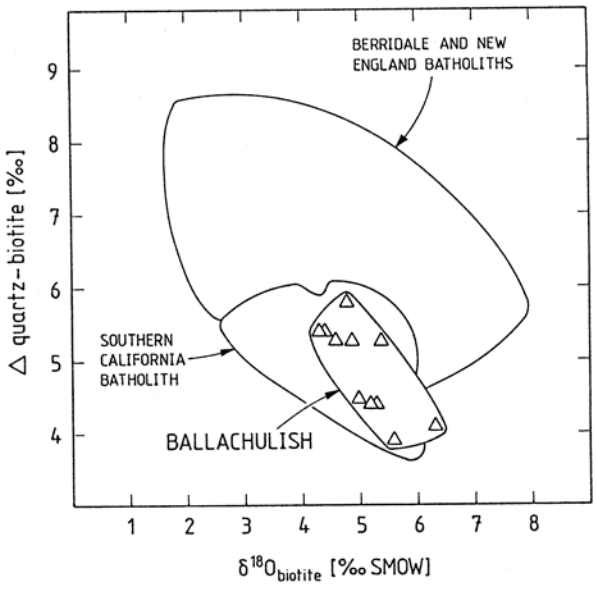

Fig. 17.5. Plot of $\Delta^{18}O_{quartz\text{-}biotite}$ vs $\delta^{18}O_{biotite}$, comparing the Ballachulish igneous complex (denoted by *triangles*) with plutonic granitoids in southeastern Australia (O'-Neil and Chappell 1977; O'-Neil et al. 1977) and western North America (Turi and Taylor 1971). These normal quartz-biotite fractionations are indicative for subsolidus isotopic exchange during cooling in the absence of meteoric hydrothermal fluids

exchange with a meteoric, hydrothermal fluid. Nabelek et al. (1983) have recognized the isotopic effects on a magma of vapor exsolution during crystallization from their detailed study of $^{18}O/^{16}O$ and D/H variations in the Notch Peak granitoid stock in Utah, USA. In the section which follows, we make direct comparison of the Ballachulish and Notch Peak intrusions, both of which are composite plutons emplaced into metasedimentary country rocks at comparable depths in the crust, to illustrate the different geological processes that may operate in the plutonic environment.

Figure 17.6a is a plot of whole-rock δD values vs whole-rock $\delta^{18}O$ values. In contrast to the Notch Peak situation, where δD variations are large relative to $\delta^{18}O$ variations, at Ballachulish $^{18}O/^{16}O$ ratios are substantially more variable than D/H ratios and no clear differences in isotopic composition are observed for the two phases of intrusion. However, the Ballachulish can be divided into three groups, on the basis of combined δD-$\delta^{18}O$ systematics and position in the intrusive complex. The first group (group A in Fig. 17.6a) consists of granites with δD = –52 to –48‰ and $\delta^{18}O$ = +9.3 to +10.9‰. These six D-rich granites are those that have been subject to extensive secondary alteration that produced chlorite after biotite, sericitization of plagioclase, and oxidation of orthoclase. Two of these samples also contain calcite veinlets (DP-462 and DP-219) and two other samples contain mineralized quartz

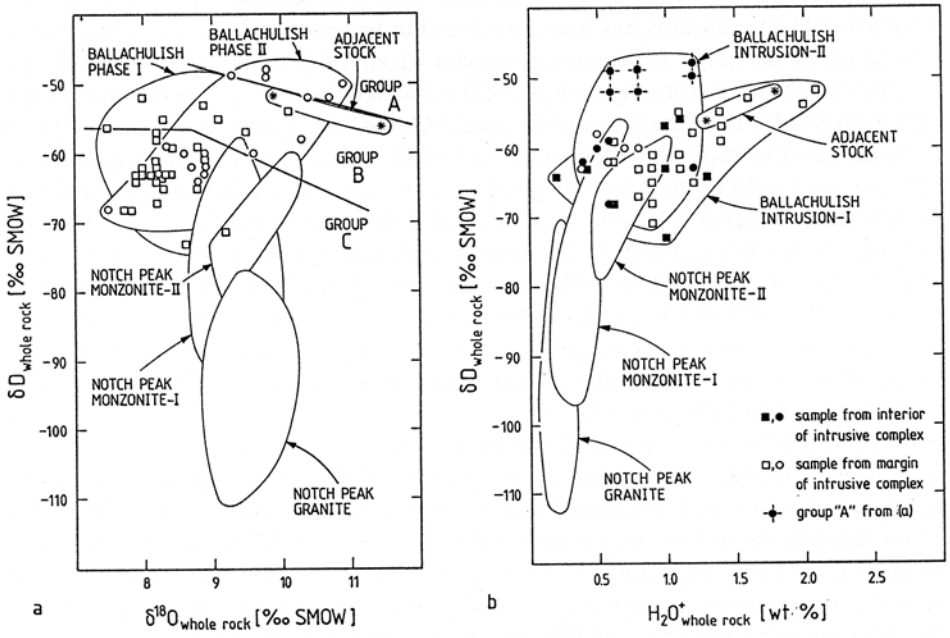

Fig. 17.6. Plots of **a** whole-rock $\delta^{18}O$ values versus whole-rock δD values, and **b** whole-rock δD values vs H_2O^+ contents. Comparison of the Ballachulish data with that of the Notch Peak stock, a Jurassic pluton of similar size and geological setting in southwestern Utah (USA), illustrates clear differences in isotopic composition and water content. *Squares* denote rocks of the intrusive phase I and *circles* denote the granitic rocks of phase II. *Asterisks* label samples of the separate stock SE of the main Complex. See text for discussion

Graham et al. (1987) for chlorite, the hydrogen isotope compositions of coexisting fluids can be calculated from the δD mineral data in Table 17.3, if the temperature of the equilibration is known. Similarly, fluid $\delta^{18}O$ values can be calculated from the mineral data in Table 17.2 using the relationships compiled in Friedman and O'Neil (1977) or more recently in O'Neil (1986), or using calculated fractionations as described by Richter and Hoernes (1988). The calculated isotopic compositions of fluids in equilibrium with hornblende and biotite at 500 °C, chlorite at 400 °C, and mineralized vein quartz fluid inclusion waters at 350–450 °C are plotted in Fig. 17.9 (see also Table 17.5). Shown for comparison are the fields generally assigned to 'primary magmatic waters' (PMW), 'normal' igneous hornblendes and biotites, and 'metamorphic waters' (Sheppard et al. 1969; Sheppard 1986), as well as the 'meteoric water line' of Craig (1961). Importantly, fluids at Ballachulish in equilibrium with hornblende fall within the field for magmatic fluids, whereas those for biotite and chlorite are displaced to significantly higher δD values. A fluid component derived from the local D-rich metasedimentary country rocks by exchange during the alteration of biotite and the formation of chlorite cannot be excluded. However, it is more likely that the high δD values of the late-stage alteration phases reflect D enrichment in residual magmatic fluids, particularly in intrusion II, resulting from both the crystallization of D-depleted hornblende and biotite (Fig. 17.7) and the progressive migration of D-rich exsolved fluids toward the centre of the magmatic complex as

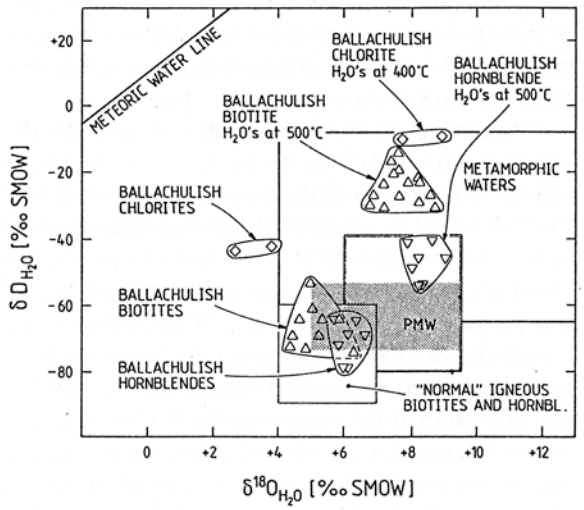

Fig. 17.9. Plot of δD and $\delta^{18}O$ values calculated for fluids in equilibrium with biotite, hornblende, and chlorite. Symbols used are as follows: ∇, Hornblende; ∇, H^2O in equilibrium with hornblende at 500 °C; Δ, Biotite; Δ, H^2O in equilibrium with biotite at 500 °C; ◊, Chlorite; ◊, H^2O in equilibrium with chlorite at 400 °C. The designations *MWL* and *PMW* refer to the "meteoric water line" (Craig 1961) and the field of "primary magmatic water" (Sheppard et al. 1969), respectively. The *shaded area* indicates the possible compositions of mineralizing fluids from fluid inclusion H-isotope and vein-mineral O-isotope analysis (Table 17.5). No evidence is observed for extensive involvement of meteoric hydrothermal fluids